ELSEVIER

Journal of Alloys and Compounds 356–357 (2003) 73–79

Journal of ALLOYS AND COMPOUNDS

www.elsevier.com/locate/jallcom

Energetics, electric-field gradients and optical properties of YH_3 (YD_3) by first-principles calculations

W. Wolf[a], P. Herzig[b,*]

[a]*Materials Designs s.a.r.l., 44 av. F.-A. Bartholdi, 72000 Le Mans, France*
[b]*Institut für Physikalische Chemie, Universität Wien, Währinger Strasse 42, A-1090 Vienna, Austria*

Received 17 July 2002; accepted 15 November 2002

Abstract

The exact crystal structure of the switchable mirror material YD_3 is still not fully understood. Presently, three structure models with $P\bar{3}c1$, $P6_3cm$, and $P6_3$ symmetry are under discussion. While the first two structures are supported by neutron powder diffraction experiments, the latter one was derived by ab-initio methods. In this paper the phase stability of these structures is established by geometry optimization and accurate total energy calculations from first-principles. The $P6_3$ structure is obtained with lowest energy followed by the $P6_3cm$ structure and the latter followed by the $P\bar{3}c1$ structure. However, these results are not decisive enough for definitive structure assignments because of the very small energy differences involved. Comparison of experimental and calculated electric-field gradients (EFGs) reveal best agreement for the $P6_3cm$ structure. From band-structure calculations it is found that within standard density-functional theory the $P\bar{3}c1$ and $P6_3cm$ structures are obtained as metals whereas for the $P6_3$ structure a small fundamental gap of ca. 1 eV results. Calculations within the screened-exchange local-density approximation (sX-LDA) lead to fundamental band gaps of 1.8–2.1 eV for all three structures.

Keywords: Metal hydride; Crystal structure; Electronic band structure; Electric field gradient; Band gap

1. Introduction

As for lanthanum and the rare-earth metals, also for yttrium a metal–insulator transition is observed in the Y–H(D) system [1] for hydrogen concentrations slightly smaller than in stoichiometric $YH(D)_3$. Although this has been well known for quite some time [2–4], the discovery by Huiberts et al. [5] that films of YH_3 and LaH_3 can be used as switchable mirrors at ambient temperatures has led to renewed interest in these compounds. Despite careful attempts to determine the exact crystal structure for $YH(D)_3$ from neutron-powder-diffraction experiments a final solution of this problem has not yet been obtained. Originally the HoD_3 structure was attributed to YH_3 [6,7]. This structure is derived from the LaF_3 structure where all octahedral F atoms lie exactly in the planes of the metal atoms. In the HoD_3 structure, which has the space group $P\bar{3}c1$, two thirds of the H atoms are shifted towards positions slightly above and below the metal planes. In the course of more recent investigations, a displacement of the hydrogen atoms from their ideal positions has been observed by Udovic et al. [8]. This shift of the H atoms has been found to be energetically favourable [9]. There is a slightly different non-centrosymmetric structure with space group $P6_3cm$ that is also compatible with the neutron-diffraction data obtained by Udovic et al. [10,11]. A further structure proposal by Kelly et al. [12] does not originate from neutron-diffraction measurements but was derived from ab-initio molecular dynamics calculations for a structure with an even further reduced space group symmetry $P6_3$. This structure is energetically slightly more favourable than the $P\bar{3}c1$ structure and leads to a small band gap of 0.8 eV even within the local-density approximation (LDA) but does not seem to be in agreement with neutron-diffraction results [13,14]. In the structures with $P6_3cm$ and $P6_3$ symmetry all octahedral H atoms are shifted out of the metal plane although their arrangement is different [11,15].

In order to solve the structure problem a few different approaches have been chosen so far. Kierey et al. [16] investigated the first-order Raman spectra of YH_3 and

*Corresponding author. Fax: +43-1-4277-9524.
E-mail address: peter.herzig@univie.ac.at (P. Herzig).

0925-8388/03/$ – see front matter
doi:10.1016/S0925-8388(03)00103-8

YD_3. They found that the number of A_1 modes observed by them is not compatible with a $P\bar{3}c1$ structure. However, their findings seem to be in agreement with the non-centrosymmetric $P6_3cm$ and $P6_3$ structures. In another approach, van Gelderen et al. [15] compared the calculated phonon densities of states for the $P\bar{3}c1$ and $P6_3$ structures to results from neutron vibration spectroscopy. These authors found better agreement for the broken symmetry ($P6_3$) structure than for the $P\bar{3}c1$ structure.

Following a different line, Herzig et al. [17] and Żogał et al. [18] used the electric-field gradients (EFGs) for D in YD_3 to draw conclusions about possible structure models by comparing the experimental results with results calculated for the $P\bar{3}c1$ and $P6_3cm$ structures. It turned out that a better agreement is found for the latter of the two structures in accordance with Kierey et al. [16].

In a very recent paper [19] the present authors investigated the phase stabilities of the three model structures by geometry optimization via minimization of the atomic forces and stress tensors and total energy calculations. The EFGs for Y and D were then calculated for the three model structures using the optimized structural parameters. Whereas standard density functional theory (DFT) [20,21] is very suitable to derive the above results, the band gap for the $P6_3cm$ structure of YH_3 was calculated on the basis of the screened-exchange local-density approximation (sX-LDA) [22,23] to overcome well-known limitations of DFT to predict electronic excitations. The results of the phase stability study and EFG calculations relevant for a structure assessment are reviewed briefly in the present paper. For computational aspects and detailed analysis the reader is referred to Ref. [19]. Since the optical appearance of YH_3 and its dramatic change with decreasing hydrogen contents is the property most relevant for applications as switchable mirrors, a detailed knowledge of the optical properties and its electronic origin is valuable. To this end, the remainder of this paper provides a comparative analysis of the band structure, band gaps and optical properties as calculated for the three model structures with $P\bar{3}c1$, $P6_3cm$ and $P6_3$ symmetries.

2. Structure optimization and total energies

In order to investigate the relative phase stabilities of the three structures (with $P\bar{3}c1$, $P6_3cm$, and $P6_3$ symmetry) total energy calculations were performed using the Vienna ab-initio simulation package (VASP) [24–26]. By this method the Kohn–Sham equations of density-functional theory [20,21] with periodic boundary conditions are solved within a plane wave basis set with electron–ion interactions described by the projector augmented wave (PAW) method [27,28]. For exchange and correlation, the generalized gradient approximation (GGA) [29] was applied. The structural parameters were calculated by atomic forces and stress-tensor minimization. Two different energy cut-offs for the plane-wave basis were applied, one corresponding to a typical ('normal basis') and the other to a highly converged set-up ('huge basis'). Table 1 shows that both levels of convergence lead to practically the same results for the phase stability hierarchy. For the $P\bar{3}c1$ structure two different sets of experimental structural parameters have been used as starting geometries. The optimization procedure should yield identical results for both, and the discrepancy arises from the imposed tolerance level. The lowest energy is found for the $P6_3$ structure followed by the $P6_3cm$ and finally by the $P\bar{3}c1$ structure. The total energy differences are very small (ca. 0.01 eV per unit cell of six formula units). Therefore, these results give some indications as regards stability but do not provide enough evidence for making decisive structure assignments at room temperature.

Table 1
Total energy per unit cell (six formula units) in eV relative to the total energy of the $P6_3$ structure for the calculated lattice parameters. The values in brackets refer to a slightly different starting geometry

Structure	Normal basis	Huge basis
$P\bar{3}c1$	0.0208 (0.0218)	0.0214 (0.0215)
$P6_3cm$	0.0095	0.0119
$P6_3$	0.0	0.0

The structural parameters for the converged set-up have been used to calculate the EFGs for the three model structures.

3. Electric-field gradients

The all-electron band-structure calculations for the calculation of EFGs are based on the density-functional theory [20,21] (DFT) and the local-density approximation and have been performed by the linearized augmented plane-wave (LAPW) method [30] in its full-potential version [31–34] (FLAPW) using an exchange-correlation potential by Hedin and Lundqvist [35,36]. For further computational details see our recent paper [19].

The EFGs have been calculated from the $l = 2$ components of the Coulomb potential near the nuclei. The formalism by Herzig [37] and Blaha et al. [38] has also been employed to split the calculated EFG components into the contributions from the surrounding electrons within the respective muffin-tin sphere ('sphere contribution') and the remainder that comes from outside this sphere ('lattice contribution'). This partitioning depends, to a small extent, on the choice of the muffin-tin radii. The valence contribution can be split further into the allowed ll' contributions (only sd, pp, dd are important in the present context) which provide useful information about the influence of particular l-like wave functions on the EFGs [39]. As is common practice the EFG component with the largest absolute value is always designated as V_{zz}.

The comparison of calculated and experimental EFGs is useful, because in this way structure models can be excluded for which the EFGs do not match. The following experimental investigations are available. Using ^{181}Ta-doped YH_3 in perturbed angular correlation (PAC) measurements [40] the EFG at the Y site has been obtained. A direct EFG determination for Y is not possible because ^{89}Y, the only naturally occurring isotope, has a nuclear spin of 1/2. NMR measurements for the D atoms in YD_3 have been performed by Balbach et al. [41] and by Żogał et al. [18] although explicit EFG values are given only by the latter authors.

As far as theoretical EFG calculations are concerned, results for the D atoms in YD_3 are presented in Refs. [17,18] and, together with results for the Y site, also in Ref. [19].

The EFGs for the relaxed structures with symmetries $P\bar{3}c1$, $P6_3cm$, and $P6_3$ and the experimental EFG values for YD_3 are presented in Table 2 (it should be noticed that only the absolute values of V_{zz} are obtained from the experimental measurements). For the calculated results for the unrelaxed $P\bar{3}c1$ structures (models I and II as designated by Udovic et al. [8]) and the $P6_3cm$ structure see Ref. [18]. For both investigations, based on the experimental [18] and optimized structural parameters [19], agreement is found to be best for the $P6_3cm$ structure. Only for the latter structure the averaged η values for D(t) are within the experimental error bar. It is noted, however, that the asymmetry parameters are quite sensitive on the small structural differences between the experimental and relaxed geometries. The calculated η values are too high for the D(t) atom in the $P\bar{3}c1$ structure and one of the D(t) atoms in the $P6_3$ structure. A comparison of the values for the Y EFG seems to be in favour of the $P6_3cm$ and the $P6_3$ structure. However, the results obtained from PAC measurements [40] studying the QI in ^{181}Hf-doped YH_3 have to be considered with care because of the probable trapping of hydrogen by the relatively high concentrations (0.5 at.%) of Hf and its daughter product Ta. New experiments would therefore be desirable to get more reliable information.

The EFG results shall be discussed although full details have been given in our recent paper [19]. For this purpose the splitting of the sphere contribution to the calculated EFGs into ll'-like contributions is required. The corresponding results for the Y atom in the different model structures are displayed in Table 3. The following interesting features are noticed.

Table 3
Split of the Y EFGs for YD_3 into their main components, i.e. pp, dd, and semicore pp. The V_{zz} values are in units of 10^{20} V/m^2

Structure model	V_{zz}	V_{zz}^{pp}	V_{zz}^{dd}	$V_{zz}^{pp(sc)}$
$P\bar{3}c1$	23.0	40.2	5.0	−22.1
$P6_3cm$	22.7	40.4	5.0	−22.6
$P6_3$	23.3	40.5	4.9	−22.2

For the Y EFG the ll' components are almost the same for all three structures. The dd components are smaller than the corresponding pp components [39] which are the largest contributions to V_{zz}. While for the valence electrons the principal axes and the corresponding ll' components are determined by the arrangement of the neighbouring atoms, this does not apply for the semicore electrons. For them, polarizing effects of the valence electrons are important. For the semicore pp components of Y this leads to opposite signs for the valence and semicore EFG components, because in this way an energetically and electrostatically favourable arrangement is reached.

Finally, the D EFGs are discussed. The results are very similar for the different structure models, but striking differences exist between the tetrahedral and octahedral D atoms. Larger negative V_{zz} values belong to the octahedral D atoms with their Y neighbours at ca. 2.14 Å and smaller negative or positive values to the tetrahedral D atoms whose nearest Y neighbours are about 2.27 Å apart. In contrast to the Y atoms with their negligible lattice contributions, for the D atoms the lattice contributions are much larger than the sphere contributions. Here the sphere contributions are dominated by the sd components in contrast to the Y EFGs where pp and, to a lesser extent, dd are the main components. As an example, the EFG components for one of the tetrahedral deuterium atoms for the $P6_3cm$ structure shall be given. The total V_{zz} value is -2.29×10^{20} V/m^2, the lattice and sphere contributions

Table 2
EFGs (in 10^{20} V/m^2) calculated for three different structure models compared to experimental results

Site	$P\bar{3}c1$		$P6_3cm$		$P6_3$		Experimental	
	V_{zz}	η	V_{zz}	η	V_{zz}	η	$\lvert V_{zz}\rvert$	η
Y	23.0	0.35	22.7	0.54	23.3	0.51	29.0	0.8
D(t)	−1.9	0.80	−2.3	0.50	−2.2	0.63	2.3	0.59±0.05
			1.7	0.62	2.0	0.84		
D(m)	−5.6	0.0	−5.2	0.0	−5.2	0.0	5.6	0.0
	−5.1	0.0	−5.2	0.0	−5.3	0.0		
					−5.2	0.0		

are -3.32×10^{20} and 1.09×10^{20} V/m^2, respectively, and the latter value has an sd component of 0.87×10^{20} V/m^2.

4. Optical properties

It was the optical appearance of YH_3 and its dramatic change with decreasing hydrogen contents that initiated renewed interest in the underlying metal–insulator transition and that opened up promising applications for switchable mirrors. A detailed study of the optical properties by means of ab-initio methods is thus desired, and comparison of possible optical transitions for different model structures may provide an additional criterion for structure determination.

Electronic band-structure calculations have been published exclusively for the $P\bar{3}c1$ symmetry and simpler structures no longer considered as realistic structure models. Standard density-functional studies did not confirm the semiconducting state but rather yielded a band overlap of 0.7–1.3 eV [9,42–44]. Optical experiments, however, measure an optical band gap of 2.3–2.8 eV [5,45,46] and indicate a fundamental band gap of about 1.8 eV [5]. The most recent optical experiments specify an optical band gap of 2.63 eV and provide hints for a fundamental band gap of an energy lower by 1–1.8 eV than the optical gap [47]. The disagreement in the band gap between theory and experiment, in particular the rather large discrepancy of 3–4 eV, gave rise to a number of different speculations. Errors of this magnitude have been observed in systems where strongly correlated d electrons are poorly represented by standard DFT, suggesting that similar strong correlation effects of electrons on hydrogen sites may be responsible for the large band gap [48–50]. On the other hand, it was found by ab-initio calculations that symmetry-breaking displacements of hydrogen atoms yielding the $P6_3$ structure model are capable of decreasing the total energy, opening up a band gap of 0.8 eV even within standard DFT [12]. The remaining discrepancy to the measured optical band gap was considered to fit the usual magnitude of the failure of DFT to reproduce band gaps. Another approach to understand the optical properties of YH_3 was pursued by ab-initio quasiparticle band-structure calculations of the $P\bar{3}c1$ [42], the LaF_3 [42,51] and the BiF_3 [51] structural models within the GW approximation. This computational approach is well validated to overcome the deficiencies of DFT, reproducing band-gaps within a few tenths of an eV. For the $P\bar{3}c1$ structure a fundamental band gap of only 1.0 eV at Γ is calculated. It is, however, argued that the fundamental band gap arises from backfolding of the conduction band at K of the LaF_3 to Γ of the $P\bar{3}c1$ structure and, therefore, corresponds to a forbidden excitation that cannot be observed in the optical spectra. The first visible transition may involve the second lowest conduction state at Γ, yielding an optical band gap of 2.8 eV as observed experimentally.

So far, optical properties were studied theoretically by assuming the $P\bar{3}c1$ or simpler structures. The present contribution aims at a comparative study of band structures and optical properties for all three structure types considered, i.e. the $P\bar{3}c1$, $P6_3cm$ and $P6_3$ structures. In order to overcome the inadequacy of standard DFT to describe band gaps and optical excitations, in addition to the standard LDA the self-consistent, screened-exchange local-density approximation (sX-LDA) [22,23] as implemented in the FLAPW method [52] was applied which has proved to be very successful in predicting band gaps, band topologies and effective masses for a wide range of semiconductors [53]. In the sX-LDA approach a part of the purely local approximation to exchange and correlation is replaced by a non-local screened Hartree–Fock operator. Further computational details may be found in Ref. [19]. The LDA and sX-LDA band-structures of the $P\bar{3}c1$ and $P6_3$ structures with optimized structural parameters (converged set-up) are shown in Figs. 1 and 2, respectively. For the corresponding band structures for the $P6_3cm$ structure obtained by an identical computational set-up we refer to Ref. [19]. The fundamental band gaps and the gap for the second excitation are listed for all three structures in Table 4.

Whereas the LDA band structures for the $P\bar{3}c1$ and $P6_3cm$ structures exhibit a band overlap at the Γ point and thus have negative band gaps of about -0.7 eV, the $P6_3$ structure indeed shows a positive band gap of 1.0 eV and thus is a semiconductor even within LDA, as already demonstrated by Kelly et al. [12]. Whereas for the first two structures the valence and conduction bands belong to different irreducible representations and thus are allowed to cross, in the broken symmetry structure the corresponding bands belong to the same irreducible representation. Consequently, band crossing is forbidden and a band gap has to open up for symmetry reasons. The fact that the bands approach each other very closely in the gap region results in the quite unusual inverse curvature of bands around the Γ point. Turning on the non-local screened interaction within sX-LDA in general causes valence and conduction bands to be pulled apart and thus removes the band overlap for the $P\bar{3}c1$ and $P6_3cm$ structures. It is quite amazing that for all three structure types the sX-LDA band structures are very similar in the whole energy range, and the peculiar features of the $P6_3$ structure model within the LDA have disappeared. Also the fundamental band gaps are almost of the same magnitude, i.e. in the range between 1.8 and 2.1 eV. The same is true for the gap of 2.9–3.0 eV bridging the second highest excitation, which is close to the optical band gap reported from transmission and reflectance experiments. Therefore, the $P6_3$ structure is not better suited to explain the optical properties than the other candidate structures. Because of the small energy differences that are within the estimated errors of the applied

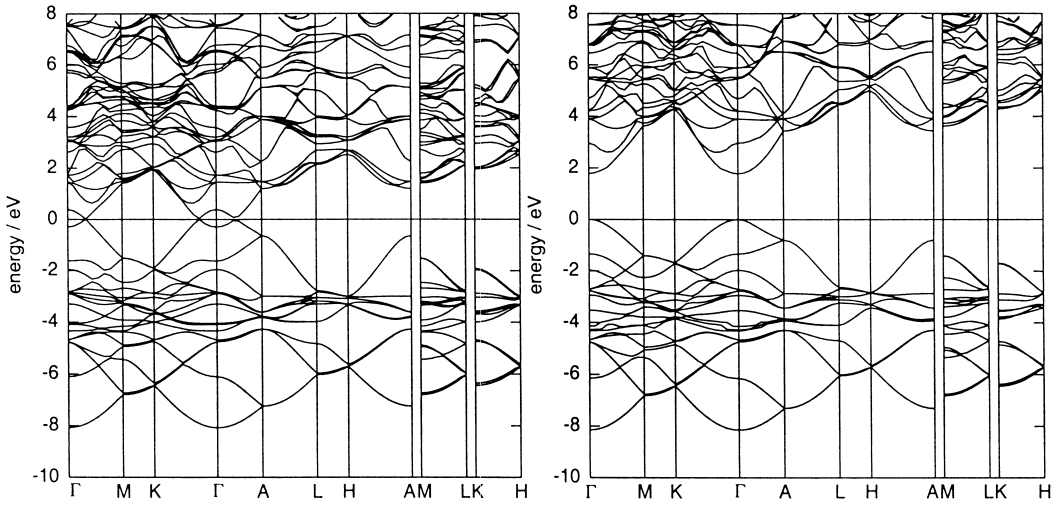

Fig. 1. Electronic band structure for YH_3 (space group $P\bar{3}c1$). Left, LDA; right, sX-LDA.

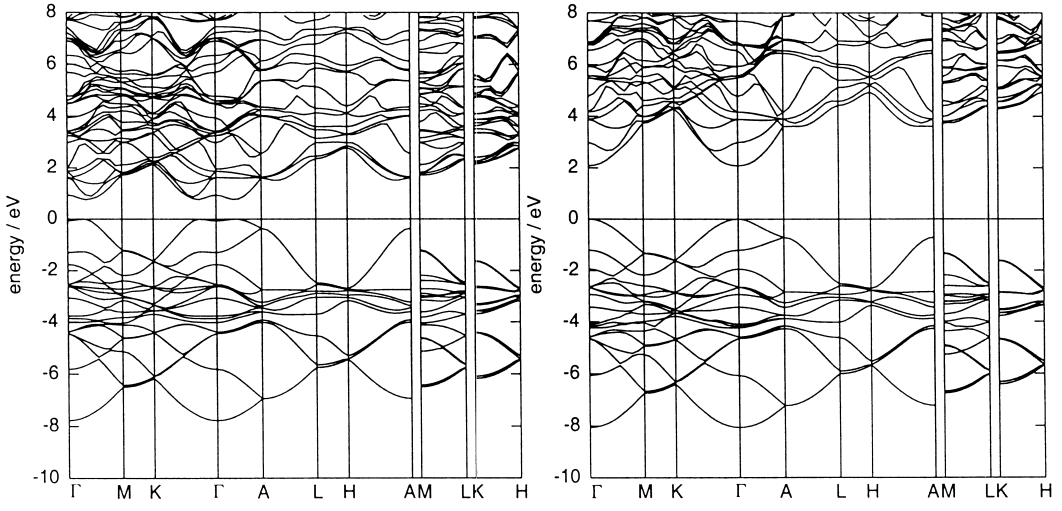

Fig. 2. Electronic band structure for YH_3 (space group $P6_3$). Left, LDA; right, sX-LDA.

methods, comparison of calculated and measured optical spectra will not be suitable to discriminate between the different structure models.

Comparing the sX-LDA band structure of the $P\bar{3}c1$ structure model with the GW band structure of Ref. [42], the most obvious difference is the much smaller fundamental band gap of 1.0 eV obtained by the GW method. Part of the difference is already contained in the larger band overlap of the LDA result, the more important part, however, is a smaller band shift for the conduction band edge due to the GW approach. Nevertheless, both methods yield the second conduction state at Γ located about 2.8–3.0 eV above the valence band edge. It seems, however, that the origin, curvature and characteristics of this band might be entirely different for both computational approaches.

Table 4
Fundamental band gap and gap of second excitation (E_2; presumably optical band gap) of YH_3 as calculated within LDA and sX-LDA for three different structure models in eV

Structure model	LDA		sX-LDA	
	E_g	E_2	E_g	E_2
$P\bar{3}c1$	−0.68	1.07	1.78	2.97
$P6_3cm$	−0.68	1.05	1.86	2.92
$P6_3$	1.00	1.68	2.09	3.00

For a unique identification of optically active transitions we systematically calculated the optical matrix elements for transitions at and in the vicinity of the Γ point within the sX-LDA approach for the three different structure models. For the higher symmetry structures $P\bar{3}c1$ and $P6_3cm$ the matrix elements of transitions corresponding to the fundamental band gap as well as those for the second highest excitation so far considered as responsible for the optical absorption edge are almost vanishing. In the vicinity of the Γ point the first large oscillator strengths are calculated for excitations of at least 4–5 eV. The situation

is somewhat different for the broken symmetry structure $P6_3$. Due to its lower symmetry most of the transitions are not symmetry forbidden any more and non-zero oscillator strengths are found for most of the transitions in the gap region. However, the oscillator strengths are about an order of magnitude smaller than those at higher energies mentioned above.

Summarizing, all three model structures are in accordance with data from optical experiments if the sX-LDA approach is applied. However, based on the three structural models and our computational approach we are not able to provide clear and definite evidence for the optical transitions involved in the absorption and reflection processes, because most of the transitions of relevant energies exhibit rather small oscillator strengths. It is noted, however, that symmetry lowering effects caused by off-stoichiometry or impurities may contribute considerably to the experimentally measured optical characteristics.

5. Concluding remarks

The structure of semiconducting YD_3, which is also of great interest for being a switchable-mirror material, is still not completely known. We have therefore performed structure optimizations and total-energy calculations based on the density-functional theory for three candidate structures. Due to the very small total-energy differences between the investigated model structures no final structure assignment is possible. For the optimized structures EFG calculations have been performed. The comparison of the calculated D EFGs with experimental results obtained from NMR measurements show best agreement for the structure with $P6_3cm$ symmetry. Based on an approach beyond DFT being suitable to treat electronic excitations, band structures and optical matrix elements have been calculated for the three candidate structures to explore the optical properties. Within this approach the band structures are very similar and are in accordance with available optical measurements. Because of the similar results for the three structures, comparison to optical experiments does not seem to be suitable for structure assessments.

Acknowledgements

The authors would like to thank P. Vajda and O.J. Żogał for stimulating discussions and the Hochschuljubiläumsstiftung der Stadt Wien (Project H-44/99) for financial support.

References

[1] P. Vajda, in: K.A. Gschneidner Jr., L. Eyring (Eds.), Handbook on the Physics and Chemistry of Rare Earths, Vol. 20, Elsevier, Amsterdam, 1995, p. 207.
[2] W.M. Mueller, in: W.M. Mueller, J.P. Blackledge, G.G. Libowitz (Eds.), Metal Hydrides, Academic Press, New York, 1968, p. 384.
[3] G.G. Libowitz, Ber. Bunsenges Phys. Chem. 76 (1972) 837.
[4] G.G. Libowitz, A.J. Maeland, in: K.A. Gschneidner Jr., L. Eyring (Eds.), Handbook on the Physics and Chemistry of Rare Earths, Vol. 3, North Holland, Amsterdam, 1979, p. 299.
[5] J.N. Huiberts, R. Griessen, J.H. Rector, R.J. Wijngaarden, J.P. Dekker, D.G. de Groot, N.J. Koeman, Nat. (Lond.) 380 (1996) 231.
[6] A. Pebler, W.E. Wallace, J. Phys. Chem. 66 (1962) 148.
[7] N.F. Miron, V.I. Shcherbak, V.N. Bykov, V.A. Levdik, Sov. Phys. Crystallogr. 17 (1972) 342;
N.F. Miron, V.I. Shcherbak, V.N. Bykov, V.A. Levdik, Kristallografiya 17 (1972) 404.
[8] T.J. Udovic, Q. Huang, J.J. Rush, J. Phys. Chem. Solids 57 (1996) 423.
[9] Y. Wang, M.Y. Chou, Phys. Rev. B 51 (1995) 7500.
[10] T.J. Udovic, Q. Huang, J.J. Rush, in: N.N. Nickel, W.B. Jackson, R.C. Bowman, R.G. Leisure (Eds.), Hydrogen in Semiconductors and Metals, Materials Research Symposium Proceedings, Vol. 513, MRS, Pittsburgh, 1998, p. 197.
[11] T.J. Udovic, Q. Huang, R.W. Erwin, B. Hjörvarsson, R.C.C. Ward, Phys. Rev. B 61 (2000) 12701.
[12] P.J. Kelly, J.P. Dekker, R. Stumpf, Phys. Rev. Lett. 78 (1997) 1315.
[13] T.J. Udovic, Q. Huang, J.J. Rush, Phys. Rev. Lett. 79 (1997) 2920.
[14] P.J. Kelly, J.P. Dekker, R. Stumpf, Phys. Rev. Lett. 79 (1997) 2921.
[15] P. van Gelderen, P.J. Kelly, G. Brocks, Phys. Rev. B 63 (2001) 100301.
[16] H. Kierey, M. Rode, A. Jacob, A. Borgschulte, J. Schoenes, Phys. Rev. B 63 (2001) 134109.
[17] P. Herzig, W. Wolf, O.J. Żogał, Phys. Rev. B 62 (2000) 7098.
[18] O.J. Żogał, W. Wolf, P. Herzig, A.H. Vuorimäki, E.E. Ylinen, P. Vajda, Phys. Rev. B 64 (2001) 214110.
[19] W. Wolf, P. Herzig, Phys. Rev. B 66 (2002) 224112.
[20] P. Hohenberg, W. Kohn, Phys. Rev. B 136 (1964) 864.
[21] W. Kohn, L.J. Sham, Phys. Rev. A 140 (1965) 1133.
[22] D.M. Bylander, L. Kleinman, Phys. Rev. B 41 (1990) 7868.
[23] A. Seidl, A. Görling, P. Vogl, J.A. Majewski, M. Levy, Phys. Rev. B 53 (1996) 3764.
[24] http://cms.mpi.univie.ac.at/vasp/;
http://materialsdesign.com/Pages/VASP.htm.
[25] G. Kresse, J. Furthmüller, Phys. Rev. B 54 (1996) 11169.
[26] G. Kresse, J. Furthmüller, Comput. Mater. Sci. 6 (1996) 15.
[27] P.E. Blöchl, Phys. Rev. B 50 (1994) 17953.
[28] G. Kresse, D. Joubert, Phys. Rev. B 59 (1998) 1758.
[29] J.P. Perdew, J.A. Chevary, S.H. Vosko, K.A. Jackson, M.R. Pederson, D.J. Singh, C. Fiolhais, Phys. Rev. B 46 (1992) 6671.
[30] O.K. Andersen, Phys. Rev. B 12 (1975) 3060.
[31] D.D. Koelling, G.O. Arbman, J. Phys. F: Metal Phys. 5 (1975) 2041.
[32] E. Wimmer, H. Krakauer, M. Weinert, A.J. Freeman, Phys. Rev. B 24 (1981) 864.
[33] H.J.F. Jansen, A.J. Freeman, Phys. Rev. B 30 (1984) 561.
[34] B.I. Min, T. Oguchi, H.J.F. Jansen, A.J. Freeman, J. Magn. Magn. Mater. 54–57 (1986) 1091.
[35] L. Hedin, B.I. Lundqvist, J. Phys. C: Solid State Phys. 4 (1971) 2064.
[36] L. Hedin, S. Lundqvist, J. Phys. (Paris) 33 (1972) C3–73.
[37] P. Herzig, Theor. Chim. Acta 67 (1985) 323.
[38] P. Blaha, K. Schwarz, P. Herzig, Phys. Rev. Lett. 54 (1985) 1192.
[39] P. Blaha, K. Schwarz, P.H. Dederichs, Phys. Rev. B 37 (1988) 2792.
[40] M. Forker, U. Hütten, M. Lieder, Phys. Rev. B 49 (1994) 8556.
[41] J.J. Balbach, M.S. Conradi, M.M. Hoffmann, T.J. Udovic, N.L. Adolphi, Phys. Rev. B 58 (1998) 14823.
[42] P. van Gelderen, P.A. Bobbert, P.J. Kelly, G. Brocks, Phys. Rev. Lett. 85 (2000) 2989.
[43] J.P. Dekker, J. van Ek, A. Lodder, J.N. Huiberts, J. Phys. Condens. Matter 5 (1993) 4805.
[44] R. Ahuja, B. Johansson, J.M. Wills, O. Eriksson, Appl. Phys. Lett. 71 (1997) 3498.

[45] R. Griessen, J.N. Huiberts, M. Kremers, A.T.M. van Gogh, N.J. Koeman, J.P. Dekker, P.H.L. Notten, J. Alloys Comp. 253–254 (1997) 44.
[46] A.T.M. van Gogh, E.S. Kooij, R. Griessen, Phys. Rev. Lett. 83 (1999) 4614.
[47] A.T.M. van Gogh, D.G. Nagengast, E.S. Kooij, N.J. Koeman, J.H. Rector, R. Griessen, C.F.J. Flipse, R.J.J.G.A.M. Smeets, Phys. Rev. B 63 (2001) 195105.
[48] K.K. Ng, F.C. Zhang, V.I. Anisimov, T.M. Rice, Phys. Rev. Lett. 78 (1997) 1311.
[49] K.K. Ng, F.C. Zhang, V.I. Anisimov, T.M. Rice, Phys. Rev. B 59 (1999) 5398.
[50] R. Eder, H.F. Pen, G.A. Sawatzky, Phys. Rev. B 56 (1997) 10115.
[51] T. Miyake, F. Aryasetiawan, H. Kino, K. Terakura, Phys. Rev. B 61 (2000) 16491.
[52] W. Wolf, E. Wimmer, S. Massidda, M. Posternak, C.B. Geller, Bull. Am. Phys. Soc. 43 (1998) 797.
[53] C.B. Geller, W. Wolf, S. Picozzi, A. Continenza, R. Asahi, W. Mannstadt, A.J. Freeman, E. Wimmer, Appl. Phys. Lett. 79 (2001) 368.